Magnetic-field-induced enhancement of ion beam energy in a magnetically expanding plasma using permanent magnets

Kazunori Takahashi, Yutaka Shida, and Tamiya Fujiwara

Department of Electrical and Electronic Engineering, Iwate University, Morioka 020-8551, Japan

E-mail: `kazunori@iwate-u.ac.jp`

Abstract. Ion energy distribution functions (IEDFs) near a source exit of a magnetically expanding argon plasma using only permanent magnets (PMs) are measured by a combination of a retarding field energy analyzer and a pulsed probe method for three types of magnetic-field configurations and various operating gas pressures, where the magnetic-field strength in the source tube is increased up to 270 Gauss by adding the number of the PM layers. The 13.56 MHz rf power for plasma production is maintained at 250 W. The IEDFs show the existence of an accelerated group of ions. It is found that the energy of the accelerated ions increases when the magnetic-field strength is increased, but saturates at seven times the electron temperature at argon pressures of 0.6-1.6 mTorr. Our results show that the maximum velocity of the accelerated ions is found to be 14 km/sec with a Mach number of 3.8.

1. Introduction

Expanding plasmas containing electric double layers (DLs) have been vigorous research subjects in connection with particle acceleration in space and laboratory plasmas, and electric propulsion devices [1, 2, 3, 4, 5, 6]. In recent laboratory experiments, supersonic ion beams accelerated by the DLs have been detected in magnetically expanding rf plasmas using retarding field energy analyzers (RFEAs) [7, 8] and laser induced fluorescence methods [9, 10, 11]. It is reported that this type of DLs is maintained by only the single plasma source, where the upstream energetic electrons overcoming the potential drop of the DL neutralize the ion beam accelerated by the DL [12, 13, 14]. The electrodeless ion acceleration mechanism is proposed to be utilized for development of a new type of electrodeless long-lifetime propulsion device [5, 15]. The previously reported ion beam energies or DL strengths were typically five times the electron temperature (5 T_e) measured at the downstream side of the DL or in the range of 3-7 T_e [4, 8, 16]. Since the thrust force of the propulsion device is related to the ion beam energy, it is important to study the detailed behavior of the ion beam energy for various conditions, e.g., the gas pressure, magnetic-field strength, rf power. Recently, the detailed role of the magnetic-field strength has been experimentally investigated by changing the solenoid currents; the ion beam energy and the DL strength are observed to increase with an increase in the magnetic-field strength in the source tube and saturate at about $5T_e$ for field strength above several tens of Gauss [17].

In studies of ion acceleration in expanding double-layer plasmas, the solenoids are used to provide the diverging magnetic field. Recently, authors have reported the generation of the supersonic ion beam in a solenoid-free plasma expanded by permanent magnets (PMs) [18, 19]. The use of the PMs would lead to a reduction of electric power consumption and of the weight of the propulsion device. The constant field region in the source tube and the diverging field region near the source exit can be created by double concentric arrays of PMs; the magnetic-field strength in the source tube was about 100 Gauss. A rapid potential drop over a thickness of 100-200 Debye length is formed near the source exit and the accelerated ion beam with energy corresponding to the potential drop is detected. In order to apply this source to the propulsion device, the detailed characteristics of the accelerated ion beam need to be investigated for various operating conditions.

In the present paper, the ion energy distribution functions (IEDFs) near the source exit of the magnetically expanding plasma using PMs are measured for three types of magnetic field strengths under various operating gas pressures, where the magnetic-field strength can be increased by adding the number of the PM layers. The enhancement of ion beam energy for strong magnetic fields is observed in the present experiments, but the energy appears to saturate at about 7 T_e for stronger magnetic fields above 200 Gauss. The maximum observed ion velocity is found to be about 14 km/sec with a Mach number of 3.8.

2. Experimental setup

2.1. Machine configuration

A schematic diagram of the experimental setup is shown in Fig. 1. A cylindrical glass tube of about 20 cm in length and 6.5 cm in inner diameter (source tube) is attached contiguously to a 26-cm-diameter and 30-cm-long grounded stainless steel vacuum chamber (diffusion chamber). The chamber is evacuated to a base pressure of 2×10^{-6} Torr by a diffusion/rotary pumping system, and the argon gas is introduced from the upstream flange of the source tube through a mass flow controller. The argon gas pressure in the vacuum chamber is maintained in the range of 0.6-1.6 mTorr, where the gas pressure is measured by the ionization gauge connected to a sideport of the diffusion chamber. A steady-state argon plasma is excited by a 7.5-cm-diameter two-turn loop antenna located at $z = -9$ cm and powered from a rf power supply of frequency 13.56 MHz and power 250 W, where $z = 0$ is defined as the interface between the source tube and the diffusion chamber. Surrounding the source tube and the rf antenna, two concentric arrays of PMs are arranged for generation of diverging magnetic-field configurations. The detailed magnetic-field configurations are described in Sec. 2.2. An insulator plate located near the upstream flange terminates the plasma cavity at the upstream side. Under these conditions, we have already reported that the rapid potential drop of the DL is spontaneously generated near the source exit ($z \sim -2$-1 cm) and the ion beam with an energy corresponding to the potential drop of the DL is detected in the downstream diffusion chamber [18]. In order to measure the IEDFs downstream of the DL, the RFEA is located at $z = 3$ cm. The RFEA consists of an electron reflector mesh biased at -60 V, an ion collector electrode, and a 3-mm-diameter entrance orifice facing the source tube. Then, the IEDF is proportional to the first derivative of the collector current I_c - collector voltage V_c curve [20], which are obtained through the pulsed probe technique [21] described in Sec. 2.3.

2.2. Magnetic-field configurations

In general, the magnetic fields produced by the PMs are strongly nonuniform with reverse-fields, i.e., cusps. According to experiments performed by Shamrai *et al.*, the cusp fields prevent the plasma diffusion, the formation of the DL, and the generation of the subsequent ion beam in the expanding plasmas [22]. Thus, it is required that the magnetic-field configuration has a constant-field region in the source tube and a diverging-field region without any cusp fields. In order to provide the above-mentioned fields, double concentric arrays of PMs as shown in Fig. 2(a) are set around the source tube. In the present experiment, all of the magnets are Neodymium Iron Boron (NdFeB) magnets of 10 cm in length, 1.5 cm in width, and 0.5 cm in thickness. All of the magnets have inward magnetization in the radial direction, i.e., in the direction of thickness. The top and the bottom of Fig. 2(b) show the side view of the sketches of the magnetic-field lines produced by the single array and the double arrays of PMs, respectively. As shown

at the top of Fig. 2(b), the single array of PMs can produce the diverging magnetic fields, but the cusp fields also exist at the axial center of the array. Between the cusp and the diverging fields, there is no constant field region for the case of the single array. On the other hand, the double arrays can create the constant field region in addition to the diverging fields as shown at the bottom of Fig. 2(b). By employing this double magnet-arrays around the source tube, the expanding magnetic fields can be applied to the machine.

In the present experiment, three types of arrangement of the magnets as shown in Fig. 3(a) are used, which are labeled as configs. (I), (II), and (III), respectively. The numbers (N_{inner}, N_{outer}) of the PMs used for the inner and outer arrays are (8, 8) for config. (I), (24, 24) for config. (II), and (24, 32) for config. (III). The calculated axial profiles of the magnetic-field strength B_z in the axial direction are plotted in Fig. 3(b) as a solid line, a dotted line, and a dotted-dashed line for configs. (I), (II), and (III), respectively. The magnetic-field strengths in the source tube for configs. (I), (II), and (III) are found to be fairly uniform and are about 100, 200, and 270 Gauss, respectively. Furthermore, it is clear the diverging magnetic fields can be provided near the source exit without any cusp fields.

2.3. Pulsed probe technique for IEDF measurement

An electronic technique for the measurement of the IEDF, i.e., the first derivative of I_c - V_c curve, is described. When the collector voltage V_c is linearly swept (dV_c/dt =constant), dI_c/dt is proportional to dI_c/dV_c, where t is time. Therefore, the IEDF can be directly obtained by the measurement of the first derivative of I_c - t characteristic when V_c is linearly swept. Figure 4(a) shows the measurement circuit of the IEDF. Outside the plasma, the current signal is passed through a resistor and then is connected to a bipolar voltage source that is swept for about 25 msec from 110 V to -40 V. The voltage signal from the resistor, i.e., the current signal, is fed through an isolation amplifier into an active analog circuit called differentiator; the detailed circuit diagram is shown in Fig. 4(b). The voltage gain G_v ($\equiv v_{out}/v_{in}$) of the circuit in Fig. 4(b) can be derived as

$$G_v = -\frac{R_2}{R_1}\frac{1}{(1 + 1/j\omega C_1 R_1)(1 + j\omega C_2 R_2)}, \tag{1}$$

$$= -\frac{R_2}{R_1}\frac{1}{(1 + 1/j\omega T)(1 + j\omega T)}, \tag{2}$$

where R_1, R_2, C_1, C_2 are the circuit parameters in Fig. 4(b), and T is defined as $T \equiv R_1 C_1 = R_2 C_2$ for simplification. In this experiment, the circuit parameters are set as $R_1 = 1$ kΩ, $C_1 = 200$ nF, $R_2 = 100$ kΩ, and C_2=2 nF, respectively. For low ($\omega T \ll 1$) and high ($\omega T \gg 1$) frequency conditions, the gain can be simplified as $G_v = -j\omega C_1 R_2$ and $G_v = -1/(j\omega C_2 R_1)$, respectively. Hence, the active circuit acts as differentiator for the current signal during slow voltage sweep and as as a filter for electric noises above a few kHz. The differentiated signal is digitized by a digital storage oscilloscope,

and passed into a LABVIEW program for conversion into ASCII data and display on a computer.

Figure 5(a) shows the representative results of the collector bias voltage V_c (dotted-dashed line), collector current I_c (dotted line), and the first derivative dI_c/dt (solid line) as a function of time t, where the data is averaged over many shots. From the data set of the measured V_c and dI_c/dt, we can obtain the IEDF shown in Fig. 5(b). The IEDF in Fig. 5(b) is found to have the bulk ions at $V_c \sim 20$ V and the accelerated group of ions at $V_c \sim 50$ V; V_c yielding these peaks in IEDF correspond to the local plasma potential ϕ_p and the beam potential ϕ_{beam}. Here, we note that the beam potential is different from the beam energy. Since V_c is the voltage from the electrical ground, zero energy corresponds to the local plasma potential, and the ion beam energy ε_{beam} can be estimated as $\varepsilon_{beam} \equiv \phi_{beam} - \phi_p$.

3. Experimental results

Figures 6(a), 6(b), and 6(c) show the normalized IEDFs measured at $z = 3$ cm for configs. (I), (II), and (III), respectively, where the argon gas pressure and the rf power are maintained at 1 mTorr and 250 W. It has previously been reported by authors that the energy of the accelerated group of ions is in good agreement with the potential difference between the upstream and downstream plasmas, where the potential drop of the DL is spontaneously generated near the source exit [18]. The local plasma potential ϕ_p and the beam potential ϕ_{beam} are indicated by solid and dashed arrows in Fig. 6. The ion beam energies $\varepsilon_{beam} = \phi_{beam} - \phi_p$ for configs. (II) and (III), i.e., for stronger magnetic-field configurations, are found to be higher than that for config. (I).

The ion beam energies ε_{beam} as a function of the argon gas pressure P_{Ar} for configs. (I), (II), and (III) are plotted in Fig. 7(a) as closed squares, crosses, and open circles, respectively. For all magnetic-field configurations, it is found that the ion beam energy increases with a decrease in the gas pressure P_{Ar}; this behavior is very similar to the previously reported results in the magnetically expanding plasmas using electromagnets, and the diffusion-controlled model [23]. Furthermore, the results in Fig. 7(a) show that the ion beam energy can be enhanced by stronger magnetic-field configurations such as configs. (II) and (III). Since there is no change of the ion beam energy between the results for configs. (II) and (III), the beam energy appears to saturate for the magnetic-field strength above about 200 Gauss.

The velocity v_{beam} of the beam ion is evaluated using [7]

$$v_{beam} = \sqrt{\frac{2e\varepsilon_{beam}}{M_i}}, \tag{3}$$

where M_i is the ion mass. The beam velocities v_{beam} obtained from the results in Fig. 7(a) are presented in Fig. 7(b); the maximum of the beam velocity is about 14 km/sec for $P_{Ar} = 0.6$ mTorr under configs. (II) and (III).

The potential drop ϕ_{DL} of the DL and the ion beam velocity are evaluated by the strength ϕ_{DL}/T_e of the DL and the Mach number, where ϕ_{DL} is observed to be equal

to the energy ε_{beam} of the ion beam. In order to discuss these values, the electron temperature T_e at the downstream side of the DL is measured at $z = 10$ cm by a single-tipped Langmuir probe, where T_e is obtained from the IV curve under the assumption of the Maxwellian electron energy distribution function (EEDF). Figure 8 shows the measured electron temperatures T_e versus the argon gas pressure P_{Ar}. The electron temperature T_e is found to be independent of the magnetic-field configuration, and decreases from about 6 eV to 3 eV when the gas pressure P_{Ar} is increased from 0.6 mTorr to 1.7 mTorr.

From the results shown in Figs. 7 and 8, ε_{beam}/T_e and a Mach number are obtained as shown in Figs. 9(a) and 9(b), respectively. Here the Mach number is derived as v_{beam}/C_s, where C_s is the ion sound speed and defined as $C_s = \sqrt{k_B T_e/M_i}$. In Fig. 9(a), ε_{beam}/T_e for various gas pressures is found to increase when the magnetic-field strength is increased to 200 and 270 Gauss, i.e., configs. (II) and (III). However, ε_{beam}/T_e corresponding to the DL strength saturates at about $7T_e$. In addition, ε_{beam}/T_e is independent of the gas pressure for configs. (II) and (III), while it is reduced from 5 to 3 for config. (I) when the pressure is increased from 0.6 mTorr to 1.6 mTorr. A possible reason for the reduction of ε_{beam}/T_e for config. (I) is that the effects of the magnetic-field would be lost in the plasma expansion for high-pressure and low-magnetic-field condition; the plasma flow becomes more diffusive and the strength of the DL triggered by the expanding magnetic field is reduced.

In a previously reported one-dimensional model of the DL in magnetically expanding plasmas, based on the sheath theory with the assumption of a Maxwellian EEDF, it has been predicted that the maximum strength of the DL is about $5T_e$ for argon plasmas [24]. Then the flux of the electrons passing through the DL is equal to the flux of the accelerated ions. According to this model, there would not be sufficient electrons overcoming the potential drop of the DL and neutralizing the accelerated ion beam if the potential drop exceeds $5T_e$. In the present experiments using the PMs, the strength of the DL is about $7T_e$, being higher than the predicted one in Ref. [24]. Moreover, the observed ion beam energy appears to be higher than the previously reported one in the magnetically expanding plasmas using electromagnets [17]. Another experiment performed in WONBAT [8] has shown the DL with the strength of $7T_e$ only for the gas pressure below 0.1 mTorr. The present experiment shows the DL strength of $7T_e$ for various gas pressures under the strong magnetic-field configurations. Although the physical mechanisms for the DL strength in the present experiment is unclear now, it is possible that the complicated magnetic-field configuration provided by the PMs could affect the potential drop of the DL and the higher-energy ion acceleration. In the present magnetic-field configuration, the magnetic-field strength is azimuthally non-uniform; hence the electrons are trapped by the magnetic fields terminated by the glass wall and heated by the rf electric fields for the plasma production. Therefore, it is possible that the energetic tail electrons is more likely in the source tube, which can overcome the potential drop of the DL and flow into the downstream plasma. Although the EEDF is treated as Maxwellian for obtaining T_e in the present experiments, the

detailed measurement of the EEDF is required in the future. In the previously reported DL plasmas using electromagnets [7], the Mach number of the accelerated ions is about 2.1, which is evaluated by the electron temperature downstream of the DL. In the present machine with the PMs, on the other hand, the maximum of the Mach number of the accelerated ion beam is found to be about 3.8. Hence, the expanding magnetic-field configuration provided by the PM arrays would be more effective for the generation of the high-speed ion beam. In addition to the above-mentioned consideration, the difference in the source diameter needs to be taken into account. The effect of the source diameter also has to be investigated hereafter.

4. Conclusion

The ion energy distribution functions (IEDFs) downstream of the double layers (DLs) are investigated in a magnetically expanding solenoid-free argon plasma using permanent magnets (PMs) under three types of magnetic-field configurations of about 100, 200, and 270 Gauss in the source tube. The IEDFs can be obtained by the combination of the retarding field energy analyzer (RFEA) and the pulsed probe technique. The IEDFs near the source exit clearly show the existence of the accelerated group of ions. The energy of the accelerated ions, which indicates the potential drop of the DL, is observed to increase with a decrease in the argon gas pressure. The energy can also be increased by increasing the upstream magnetic-field strength from previously reported 100 Gauss to above 200 Gauss in the present experiments, although the energy saturates at seven times the electron temperature. The maximum velocity of the accelerated ions is about 14 km/sec and 3.8 in Mach number.

References

[1] Hairapetian G and Stenzel R L 1988 *Phys. Rev. Lett.* **61** 1607

[2] Ergun R E, Su Y -J, Andersson L, Carlson C W, McFadden J P, Mozer F S, Newman D L, Goldman M V, and Strangeway R J 2001 *Phys. Rev. Lett.* **87** 045003

[3] Boswell R W, Marsch E, and Charles C 2006 *Astrophys. J.* **640** L199

[4] Charles C 2007 *Plasma Sources Sci. Technol.* **16** R1 and references therein

[5] Charles C 2009 *J. Phys. D: Appl. Phys.* **42** 163001 and references therein

[6] Ergun R E, Andersson L, Tao J, Angelopoulos V, Bonnell J, McFadden J P, Larson D E, Eriksson S, Johansson T, Cully C M, Newman D N, Goldman M V, Roux A, LeContel O, Glassmeier K -H, and Baumjohann W 2009 *Phys. Rev. Lett.* **102** 155002

[7] Charles C and Boswell R W 2004 *Phys. Plasmas* **11** 1706

[8] Sutherland O, Charles C, Plihon N, and Boswell R W 2005 *Phys. Rev. Lett.* **95** 205002

[9] Cohen S A, Siefert N S, Stange S, Boivin R F, Scime E E, and Levinton F M 2003 *Phys. Plasmas* **10** 2593

[10] Sun X, Keesee A M, Biloiu C, Scime E E, Meige A, Charles C, and Boswell R W 2005 *Phys. Rev. Lett.* **95** 025004

[11] Thakur S C, Harvey Z, Biloiu I A, Hansen A, Hardin R A, Przybysz W S, and Scime E E 2009 *Phys. Rev. Lett.* **102** 035004

[12] Meige A and Boswell R W 2006 *Phys. Plasmas* **13** 092104

[13] Takahashi K, Charles C, Boswell R W, Kaneko T, and Hatakeyama R 2007 *Phys. Plasmas* **14** 114503

[14] Takahashi K, Charles C, Boswell R W, and Hatakeyama R 2008 *Phys. Plasmas* **15** 074505

[15] West M D, Charles C, and Boswell R W 2008 *J. Propul. Power* **24** 134

[16] Charles C and Boswell R W 2003 *Appl. Phys. Lett.* **82** 1356

[17] Charles C and Boswell R W 2007 *Appl. Phys. Lett.* **91** 201505

[18] Takahashi K, Oguni K, Yamada H, and Fujiwara T 2008 *Phys. Plasmas* **15** 084501

[19] Takahashi K and Fujiwara T 2009 *Appl. Phys. Lett.* **94** 061502

[20] Takahashi K, Kaneko T, and Hatakeyama R 2006 *Plasma Sources Sci. Technol.* **15** 495

[21] Schoenberg K F 1978 *Rev. Sci. Instrum.* **49** 1377

[22] Shamrai K P, Virko Y V, Virko V F, and Yakimenko A I, Proceedings of the 42nd AIAA/ASME/SAE/ASEE Joint Propulsion Conference and Exhibit, California 2006, (the American Institute of Aeronautics and Astronautics, 2006), p. 4845.

[23] Lieberman M A, Charles C, and Boswell R W 2006 *J. Phys. D: Appl. Phys.* **39** 3294

[24] Chen F F 2006 *Phys. Plasmas* **13** 034502

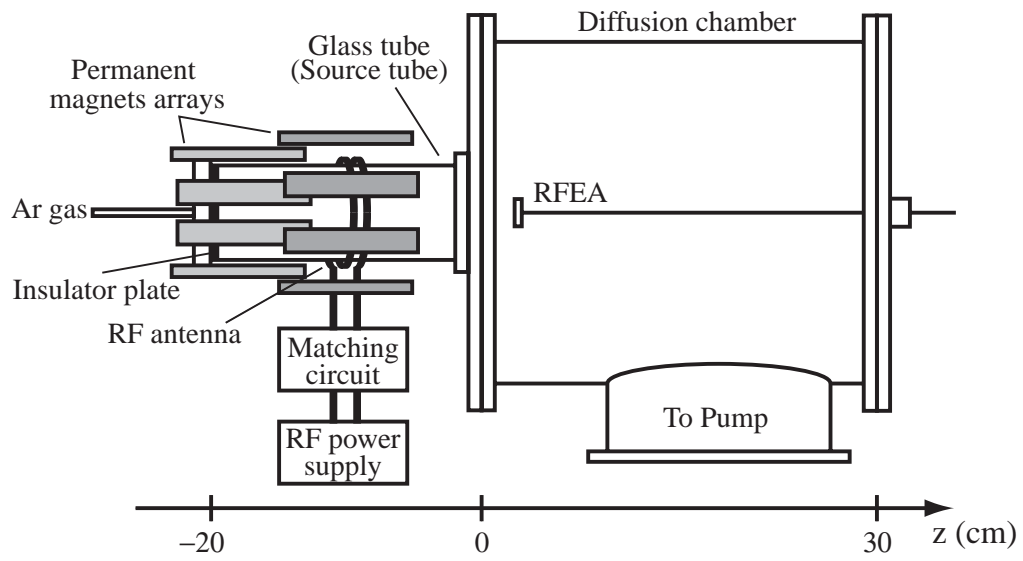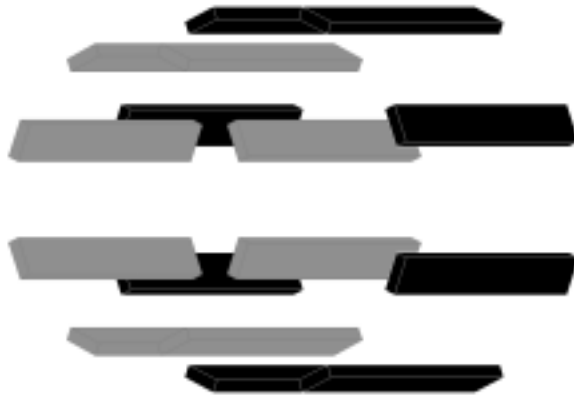**Figure 1.** Schematic of the experimental setup.

(a)

(b)

diverging fields

cusp

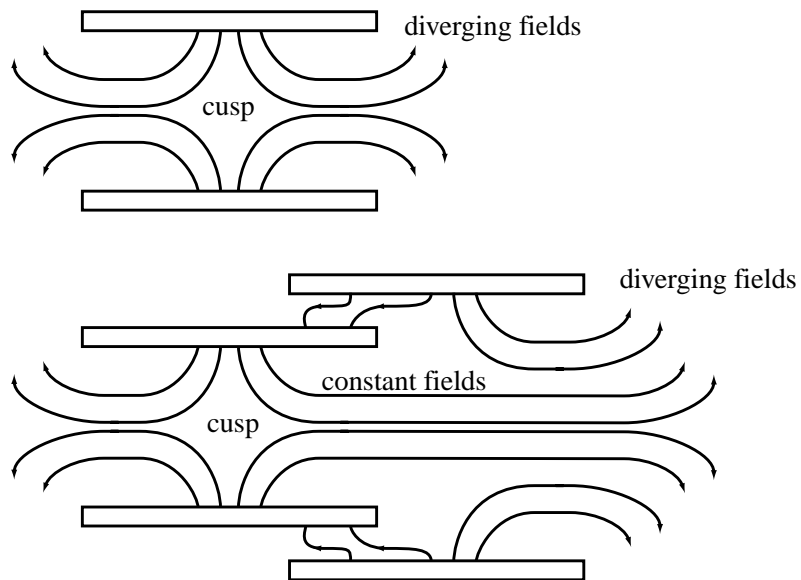diverging fields

constant fields

cusp

Figure 2. (a) Schematic view of the double concentric arrays of PMs. (b) Images of the magnetic-field lines created by the single magnet-array (top) and the double magnet-arrays (bottom).
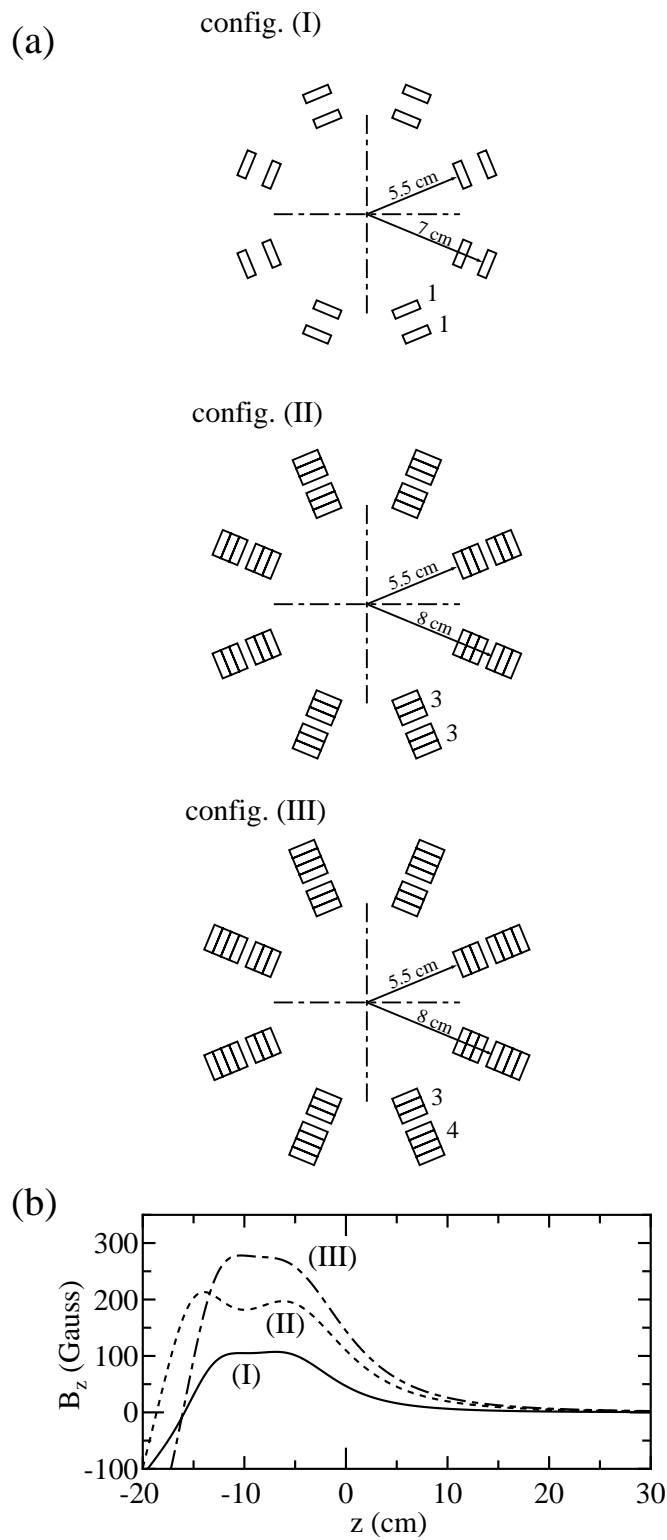
Figure 3. (a) Axial view of the three types of the PMs arrays, which are labeled as configs. (I), (II), and (III). (b) The calculated magnetic-field configurations for configs. (I) (solid line), (II) (dotted line), and (III) (dotted-dashed line).
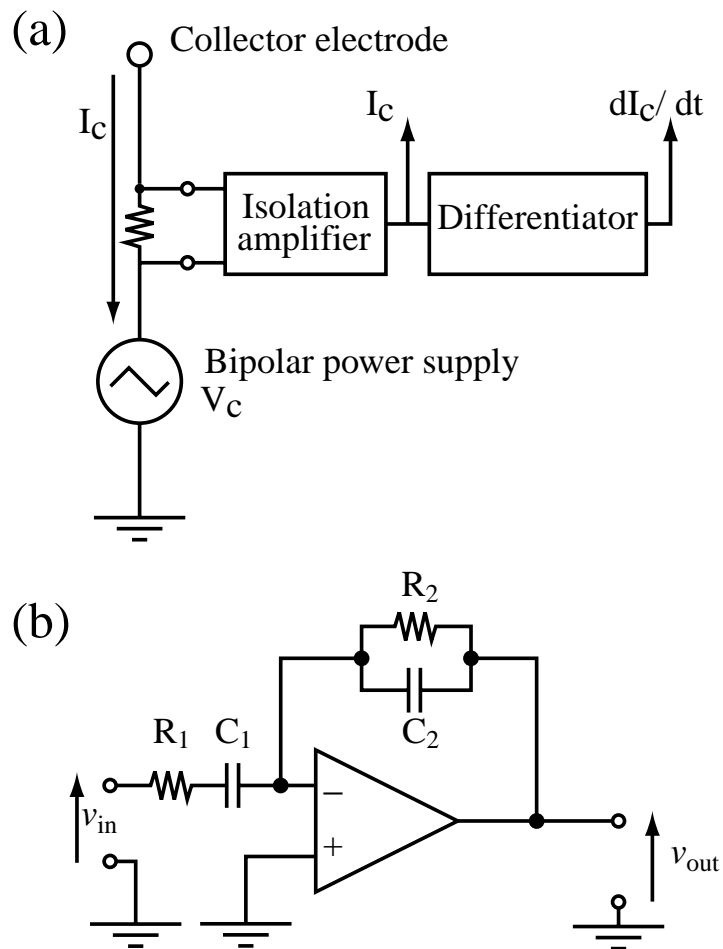
Figure 4. (a) Circuit diagram for the measurement of the IEDFs. (b) The detailed circuit diagram of the differentiator.
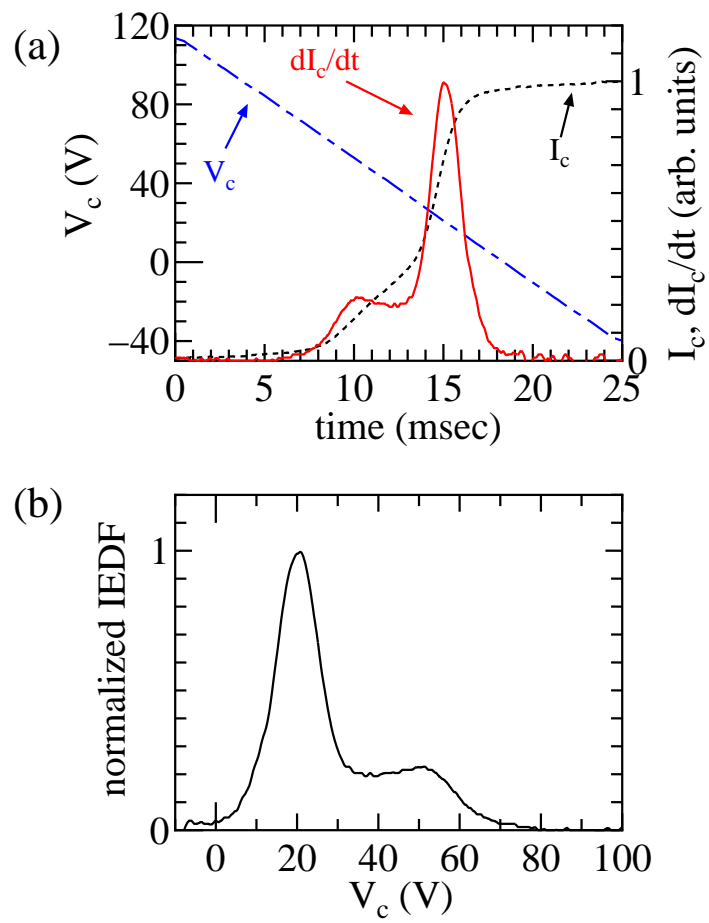
Figure 5. (a) Representative results of the collector bias voltage V_c (dotted-dashed line), collector current I_c (dotted line), and the first derivative dI_c/dt (solid line) as a function of time t. (b) Normalized IEDF obtained from Fig. 5(a).
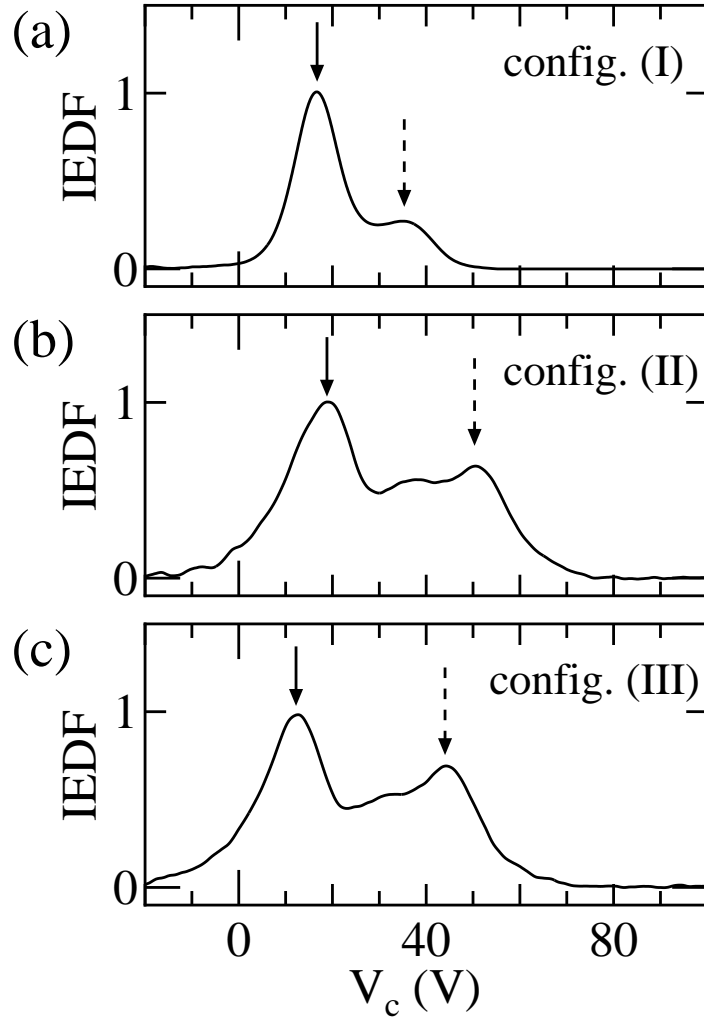
Figure 6. Normalized IEDFs at $z = 3$ for configs. (I), (II), and (III). The gas pressure and the rf power are maintained at 1 mTorr and 250 W. The solid and dashed arrows show the local plasma potential ϕ_p and the beam potential ϕ_{beam}, respectively.
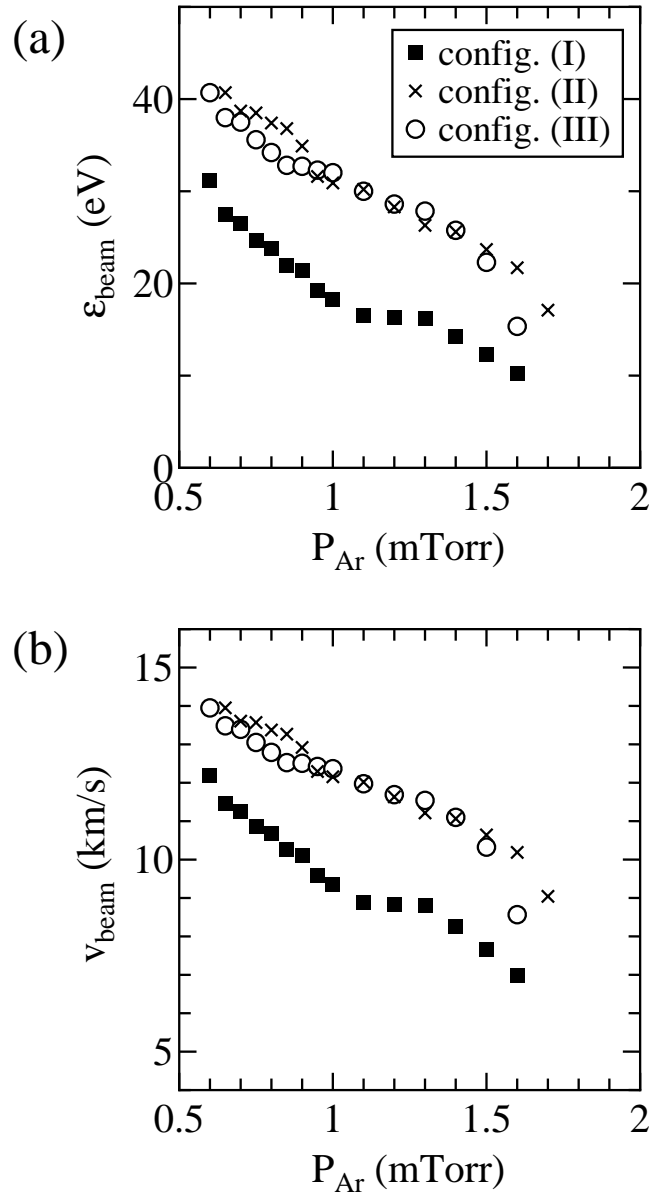
Figure 7. (a) Ion beam energies ε_{beam} and (b) ion beam velocities v_{beam} as a function of gas pressure P_{Ar} for config. (I) (closed squares), for config. (II) (crosses), and for config. (III) (open circles).
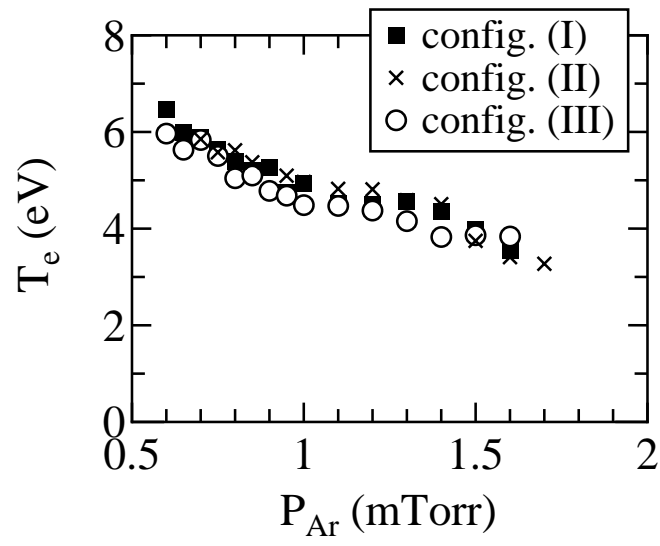
Figure 8. Electron temperatures T_e at $z = 10$ cm as a function of gas pressure P_{Ar} for config. (I) (closed squares), for config. (II) (crosses), and for config. (III) (open circles).
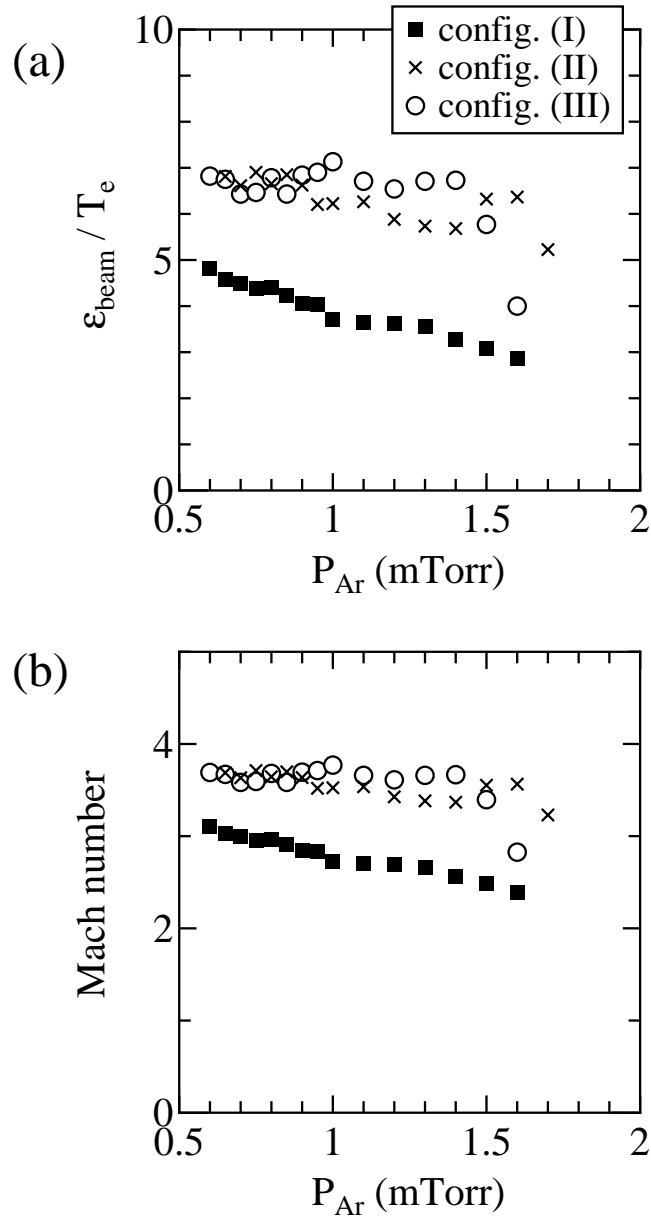
Figure 9. (a) Ion beam energies normalized by the electron temperatures ε_{beam}/T_e and (b) mach numbers, as a function of gas pressure P_{Ar} for config. (I) (closed squares), for config. (II) (crosses), and for config. (III) (open circles).